1-1-2012

Reduction of seismic pounding effects of base-isolated RC highway bridges using MR damper

M N. Sheikh
University of Wollongong, msheikh@uow.edu.au

J Xiong
University of Wollongong

W H. Li
University of Wollongong, weihuali@uow.edu.au

54379

Structural Engineering and Mechanics, Vol. 41, No. 6 (2012) 791-803

Reduction of seismic pounding effects of base-isolated RC highway bridges using MR damper

40%, 36%, 30%,

M.N. Sheikh*[1], J. Xiong[1a] and W.H. Li**[2]

[1]*School of Civil, Mining and Environmental Engineering, University of Wollongong, NSW 2522, Australia*
[2]*School of Mechanical, Materials and Mechatronic Engineering, University of Wollongong, NSW 2522, Australia*

(Received October 20, 2011, Revised February 8, 2012, Accepted February 21, 2012)

Abstract. Significant structural damages due to pounding between adjacent superstructures of multi-span reinforced concrete (RC) highway bridges have been observed in past earthquakes. Different methods have been proposed in the literature to mitigate the adverse seismic pounding effects. This paper presents an analytical investigation on the use of magnetorheological (MR) dampers in reducing seismic pounding effects of base-isolated multi-span RC highway bridges. It has been observed that MR damper can effectively reduce the seismic pounding effect. Three control strategies (passive off, passive on, and bang bang control) of MR damper have been investigated. Although all the control strategies are found to be effective, bang bang control has been observed to be the most effective.

Keywords: MR damper; pounding; highway bridges; control strategies; earthquakes

1. Introduction

Bridges are considered critical components of highway transportation network, as closure of a bridge due to partial damage or collapse can disrupt the total transportation system. However, earthquakes in the past few decades around the world have demonstrated the vulnerability of engineered bridges even in the event of a moderate earthquake.

In general, bridges lack structural redundancy and hence suffer severe damage which leads to failure during earthquakes. A more robust bridge design is not considered economical or even effective, unless earthquake induced forces in the structure are reduced by means of seismic isolation. Seismic isolation devices generally used in the bridge decouple the bridge deck from the bridge substructure and hence reduce seismic forces transmitted to abutments and piers. However, in the event of a moderate to strong earthquake ground motion, the displacement demand at the expansion joint of a base-isolated multi-span bridge can be many times higher than the clearance between the decks. The phenomenon is commonly known as seismic pounding. Pounding has been identified as the main cause of the initiation of damage and may change the seismic response of the

*Corresponding author, Senior Lecturer, E-mail: msheikh@uow.edu.au
**Corresponding author, Associate Professor, E-mail: weihuali@uow.edu.au
[a]Masters Student

entire bridge.

A number of studies have been conducted to investigate the effectiveness of structural control devices in reducing seismic pounding effect of bridges. Jankowski *et al.* (2000) investigated the use of dampers and stiffeners, rubber bumpers, crushable devices, and shock transmission units to mitigate pounding effect. Zhu *et al.* (2004) further investigated the effectiveness of such control devices by 3D non-linear modelling of a three span elevated steel bridge and observed 50% reduction in structural response. However, the proposed control devices make the bridge decks continuous and may place high force demand at bridge piers.

Magnetorheological (MR) fluids are smart materials whose rheological or mechanical properties can be rapidly and reversely controlled via an external magnetic field (Wang and Gordaninejad 2007, Li *et al.* 2002). MR damper, a semi active control device, has recently been found to be effective, based on both analytical and experimental investigation, to reduce the vibration of structures under earthquake induced ground motions (Sireteanu and Stammers 2000, Spencer *et al.* 1997). It is an intelligent device which can adjust the damping parameters by altering the magnetic field in MR fluid (Li *et al.* 2000, Yao *et al.* 2002). Guo and Li (2008) investigated the possibility of using MR damper to reduce the pounding effect of adjacent segments of highway bridges in extreme earthquake events. They designed MR damper to trace the instantaneous optimal control forces for manipulating the dampers. Later, Guo *et al.* (2009) carried out both analytical and experimental investigations (shaking table tests) on a 1:20 scaled base-isolated bridge model and proposed an optimization approach for MR damper which can effectively reduce seismic pounding effect.

The aim of this paper is to investigate whether MR damper with simple control strategies can effectively reduce the pounding effect of base-isolated multi-span RC highway bridge. A three-segment base isolated multi-span highway bridge has been modelled using MATLAB SIMULINK. Three simple control strategies namely, Passive off, passive on and bang bang control strategies have been investigated. It has been observed that even simple control strategies can effectively reduce the forces generated due to pounding of adjacent superstructure segments.

2. Modelling of pounding of base-isolated RC highway bridge

2.1 Modelling assumptions

The base-isolated highway bridge analysed in this study consists of flexible bearings with stiff piers (Section 4.1), whose stiffness is significantly higher than the stiffness of flexible bearings. The contribution of bridge pier to the dynamic response of the superstructure segment of the bridge is considered small and hence not considered. The spatial variation of earthquake ground motion is not considered critical, as the studied bridge is not very long. Hence, pounding effect is considered arising from dynamic characteristics of the bridge segments. The pounding effect between the superstructure and abutment is not considered within the scope of the paper.

2.2 Simplified modelling for pounding between adjacent superstructure segments

Pounding between adjacent superstructure segments of bridges is a complex phenomenon which may involve plastic deformation, friction, local crushing as well as fracturing at contact surfaces.

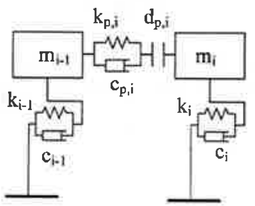

Fig. 1 Bridge pounding model based on contact element approach

Pounding forces act during time lapses that are very small compared to the natural vibration periods of the structures (Vega *et al.* 2009). Moreover, generated stress waves also propagate into the impacting bodies. Accurate modelling considering the factors described above is complicated and considered not important for the scope of this study. A simplified modelling approach for pounding between adjacent segments is considered sufficient.

Simplified modelling for pounding can be developed adopting stereo mechanical approach and contact-element approach. The analysis conducted in this study is based on contact-element approach because of its simplicity in mathematical formulation. Fig. 1 shows the schematic diagram of bridge pounding model, based on contact-element approach. It is assumed that the adjacent segments are connected by a linear spring and a damper.

$K_{p,i}$, $c_{p,i}$, $d_{p,i}$ are the linear stiffness of contact spring, the linear damping coefficient of dashpot, and the clearance between the $(i-1)$th and ith segments. Under longitudinal ground motion, the response of each segment is independent of each other, unless the relative displacement between the two adjacent segments becomes larger than the clearance between them, which is the condition of pounding. The relative displacement can be calculated as

$$\delta_{(i-1,i)}(t) = x_{i-1}(t) - x_i(t) - d_{p,i} \tag{1}$$

Where $\delta_{(i-1,i)}(t)$ is the relative displacement between the $(i-1)$th segment and the ith segment; $x_{i-1}(t)$ and $x_i(t)$ are the displacement of $(i-1)$th segment and the ith segment with respect to bridge foundation. The pounding force between the colliding superstructures can be expressed as

$$F_{p,i}(t) = k_{p,i}(t)\delta_{(i-1,i)}(t) + c_{p,i}(t)\dot{\delta}_{(i-1,i)}(t) \quad \text{for} \quad \delta_{(i-1,i)}(t) \geq 0 \tag{2}$$

$$F_{p,i}(t) = 0 \quad \text{for} \quad \delta_{(i-1,i)}(t) < 0 \tag{3}$$

where $F_{p,i}(t)$ is the pounding force between the $(i-1)$th and the ith segments of the bridge. $\dot{\delta}_{(i-1,i)}(t)$ is relative velocity between adjacent superstructure segments. The pounding effect is appeared only when the adjacent segments are in contact. So the stiffness of the linear impact spring $k_{p,i}(t)$ and the linear impact damping coefficient which describing the energy dissipation during pounding $c_{p,i}(t)$ are time dependent and can be written as

$$k_{p,i}(t) = k_{p,i}; \; c_{p,i}(t) = c_{p,i} \quad \text{for} \quad \delta_{(i-1,i)}(t) \geq 0 \tag{4}$$

$$k_{p,i}(t) = 0; \; c_{p,i}(t) = 0 \quad \text{for} \quad \delta_{(i-1,i)}(t) < 0 \tag{5}$$

The contact stiffness $k_{p,i}$ in Eq. (2) is taken proportional to the axial stiffness of the contact superstructures (Maison and Kasai 1992)

$$k_{p,i} = \frac{E_{i-1,i}A_{i-1,i}}{l_{i-1,i}} \tag{6}$$

The $E_{i-1,i}$ is the elastic modulus; $A_{i-1,i}$ is the cross section area; $l_{i-1,i}$ is the length of the deck with small axial stiffness.

The damping coefficient of the impact model is obtained from the formula suggested in Anagnostopoulos 1988.

$$c_{p,i} = 2\xi_{p,i}\sqrt{k_{p,i}\frac{m_{i-1}m_i}{m_{i-1}+m_i}} \tag{7}$$

$$\xi_{p,i} = \frac{-\ln e_{p,i}}{\sqrt{(\ln e_{p,i})^2 + \pi^2}} \tag{8}$$

where, $\xi_{p,i}$ is the damping ratio of the ith element, which is correlated with the coefficient of restitution $e_{p,i}$. m_{i-1} and m_i are the mass of the $(i-1)$th and ith segment of the superstructure. The values of $e_{p,i}$ varies from 0.5 to 0.75 (Anagnostopoulos 1988). However, pounding pattern is not significantly affected by impact element damping (Jankowski *et al.* 1998).

A base-isolated highway bridge is constituted by several superstructure segments. Each segment is assumed as a linear independent single-degree of freedom system with lumped mass. By considering the equilibrium of forces for each degree of freedom, the governing equations of motion for each superstructure segment can be obtained as

$$m_1\ddot{x}_1 + c_1\dot{x}_1 + k_1x_1 + c_{p,1}(\dot{x}_1 - 0) + k_{p,1}(x_1 - 0 + d_1) + c_{p,2}(\dot{x}_1 - \dot{x}_2) + k_{p,2}(x_1 - x_2 - d_2) = m_1\ddot{u}_{g,1}(t)$$

$$\cdots\cdots$$

$$m_i\ddot{x}_i + c_i\dot{x}_i + k_ix_i + c_{p,i}(\dot{x}_i - \dot{x}_{i-1}) + k_{p,i}(x_i - x_{i-1} + d_i) + c_{p,i+1}(\dot{x}_i - \dot{x}_{i+1}) + k_{p,i+1}(x_i - x_{i+1} - d_{i+1}) = m_3\ddot{u}_{g,i}(t)$$

$$\cdots\cdots\cdots$$

$$m_n\ddot{x}_n + c_n\dot{x}_n + k_nx_n + c_{p,n}(\dot{x}_n - \dot{x}_{n-1}) + k_{p,n}(x_n - x_{n-1} + d_n) + c_{p,n+1}(\dot{x}_n - 0) + k_{p,n+1}(x_n - 0 - d_{n+1}) = m_n\ddot{u}_{g,n}(t) \tag{9}$$

where, x_i, $\dot{x}_i$, $\ddot{x}$, are displacement, velocity and acceleration of the segment relative to the ground. $\ddot{x}_{g,i}(t)$ is the input ground motion acceleration.

By using the matrix-vector notation the governing equation of motion of the structure in the longitudinal direction with the pounding effects can be written as

$$\mathbf{M}\ddot{\mathbf{X}}(t) + [\mathbf{C} + \mathbf{C}_P(t)]\dot{\mathbf{X}}(t) + [\mathbf{K} + \mathbf{K}_p(t)]\mathbf{X}(t) + \mathbf{E}_P(t)d_P = -\mathbf{M}\ddot{\mathbf{u}}_g(t) \tag{10}$$

M is the mass matrix of the superstructure, **C** is the damping matrix of the superstructure, and **K** is the stiffness matrix of the superstructure. In this study, the damping and stiffness are from the rubber bearing used for base isolation. $\mathbf{C}_P(t)$ and $\mathbf{K}_P(t)$ are the contact damping and stiffness matrices due to pounding. $\ddot{\mathbf{X}}(t), \dot{\mathbf{X}}(t), \mathbf{X}(t)$ are the acceleration, velocity and the displacement matrices of the segment with respect to the ground. $\mathbf{E}_P(t)$ is the of pounding force matrix.

Considering installation of a MR damper, the equation of the highway bridge with the MR damper is shown in below

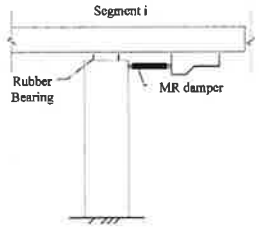

Fig. 2 MR damper between superstructure segment and the cap beam

$$\mathbf{M}\ddot{\mathbf{X}}(t)+[\mathbf{C}+\mathbf{C}_P(t)]\dot{\mathbf{X}}(t)+[\mathbf{K}+\mathbf{K}_p(t)]\mathbf{X}(t)+\mathbf{E}_P(t)d_P+\mathbf{F}_d=-\mathbf{M}\ddot{\mathbf{u}}_g(t) \quad (11)$$

where F_d is the control force generated by the MR damper. It depends on the location and the type of MR dampers. In this study MR damper has been installed between each superstructure segment and the corresponding cap beam (Fig. 2). The control force provided by the MR damper can act directly on the superstructure segment to reduce relative displacement and hence the pounding force.

3. Modelling of mr damper

3.1 Behaviour of MR damper

MR dampers, consisting of a fixed orifice damper filled with a controllable MR fluid, are semiactive control devices which offer highly reliable operation. Even in the case of malfunction, they become passive damper. Although MR damper is a highly non-linear device, a simple but appropriate model for MR damper can reliably predict the behaviour of controlled structure. Spencer *et al.* (1997) proposed a phenomenological model based on a Bouc-Wen hysteresis model, as shown in Fig. 3, which is adopted herein to predict the behaviour of wide range of hysteretic behaviour.

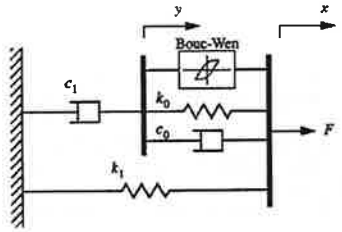

Fig. 3 Bouc-wen phenomenological model (Spencer *et al.* 2007)

The force in this system is given by

$$F = c_0\dot{x} + k_0x + \alpha z \quad (12)$$

where the evolutionary variable z is governed by

$$\dot{z} = -\gamma|\dot{x}|z|z|^{n-1} - \beta\dot{x}|z|^n + A\dot{x} \quad (13)$$

where γ, β and A are parameters related to the shape of hysteresis loop. By adjusting these parameters, the linearity in the unloading and the smoothness of the transition from the pre-yield to

Table 1 Parameters of the generalised Bounc-wen phenomenological model

Parameter	Value	Parameter	Value
c_{0a}	21 N s cm^{-1}	α_a	140 N cm^{-1}
c_{0b}	3.5 N s cm^{-1} V^{-1}	α_b	695 N s cm^{-1}
k_0	46.9 N cm^{-1}	γ	363 cm^{-2}
c_{1a}	283 N s cm^{-1}	β	363 cm^{-2}
c_{1b}	2.95 N s cm^{-1} V^{-1}	A	301
k_1	5.00 N cm^{-1}	n	2
x_0	14.3 cm	η	190 s^{-1}

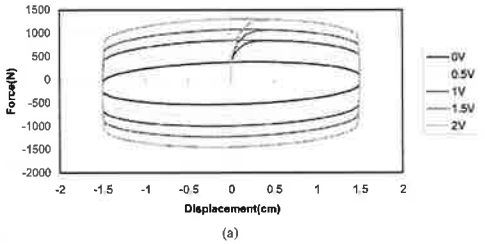

(a)

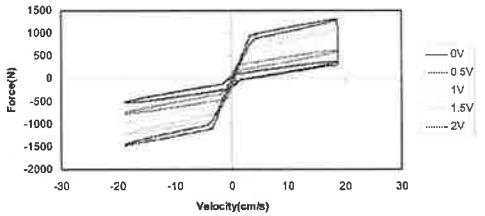

(b)

Fig. 4 The response of MR damper with 2 Hz sinusoidal excitation: (a) the relationship between displacement and force, and (b) the relationship between velocity and force

the post-yield region can be controlled. This model consists of 14 parameters, all of which were identified by the optimization algorithm available in MATLAB toolbox. One typical set of parameters are given from the tests of Spencer al et. as shown in Table 1. Based on above equations and parameters value, the force of MR damper can be calculated in different magnetic field by changing the voltage input.

Using the parameters above, the damper responses under different voltages were re-constructed and shown in Fig. 4(a) and (b). It is obvious that the model can predict the damper performance very well.

It can be observed from From Fig. 4 that with the increase of the input voltage, the damping force of MR damper increases, the area force-displacement hysteretic loop's increase and the capacity of energy consumption for MR damper increases, as well. With the increase of the velocity, the damping force of MR damper increase, because of the increase of viscous damping force. The velocity- force curve shows that the Bounc-wen phenomenal model can simulate the force output when the velocity closes to zero.

3.2 Control of MR damper

To reduce the pounding between adjacent superstructure, MR dampers are assumed to be installed between the decks and the piers of each segment. Three simple control algorithms have been chosen to be tested:

Passive off: In passive off, there is no current input to the MR device and hence there is no voltage input. As no magnetic field acts, MR fluid does not exhibit any magnetorheological properties. Effectively, MR dampers act as a passive damper.

Passive on: In this control system, the current supply and hence the voltage remains constant. In this study voltage is kept constant at 2 V.

Bang-bang control: Bang-bang control has been used for vibration control of cable bridges (Yang *et al.* 2011). The control algorithm switch between two states without any interval and is related to the displacement and velocity of the superstructure. When the displacement and velocity of the superstructure have the same direction, the stiffness and damping of the system increase and reach the maximum value (2 V). However, when the displacement and velocity of the system have different directions, the stiffness and damping of the system drop to minimum value (0 V). The control algorithm can be written as

$$V(t)=\begin{cases} V_{\max} & x_i(t)\dot{x}_i(t)>0 \\ V_{\min} & x_i(t)\dot{x}_i(t)\le 0 \end{cases} \tag{14}$$

Where, $V(t)$ is the control signal. $V_{\max}$ and $V_{\min}$ are the maximum and minimum value of the input voltage respectively.

4. Effectiveness of MR damper in reducing pounding effect

4.1 Parameter of multi-span RC highway bridge

The bridge models adopted in this study was developed based on the model originally presented

by Jankowski *et al.* (2000). A three-span bridge model has been developed for this study. Each segment consists of three equal spans of 40 m length and 14 m wide pre-stressed concrete deck with a mass of 2×10^4 kg/m. The bridge substructure consists of RC piers of equal height of 11.5 m. The bridge deck is supported by two high-damping rubber bearing. The damping ratio of the bearings is 0.14. The expansion joints between segments are taken as 0.05 m. As the contribution of the bridge pier to the total stiffness of the bridge is small, for the simplicity of the analyses, the stiffness contribution by the piers is ignored. The stiffness' of end segments and mid segment are considered as 8.15×10^7 and 7.19×10^7 N/m, respectively. Hence, the fundamental vibration periods of end segments and mid segment are 1.078 s and 1.148 s, respectively. The contact stiffness and damping coefficients are calculated as 3.475×10^9 N/m and 1.808×10^7 Ns/m, calculated based on the structural properties of the bridge (Eqs. (6)-(7)).

4.2 Input ground motion records

The 1940 El Centro (north-south components) are used to demonstrate the effectiveness of the MR damper in reducing seismic pounding effects. The earthquake records have been scaled to obtain the peak ground acceleration of 800 gal to represent the motion of a strong earthquake ground motion.

4.3 Response of the bridge without control

The base isolated three-segment RC bridge model without the inclusion of pounding effect is first analysed to evaluate the response of the uncontrolled model in the event of an earthquake shaking.

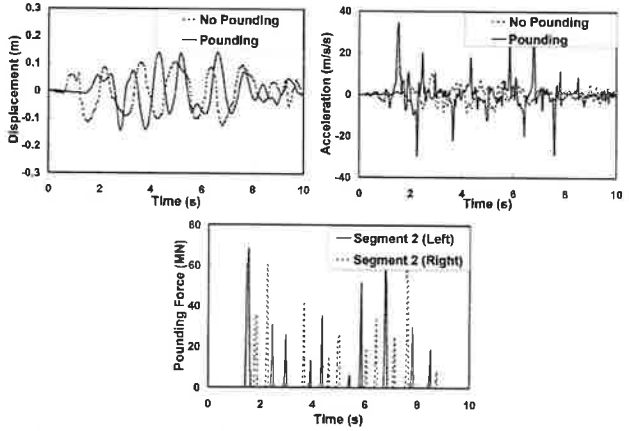

Fig. 5 Structural response of segment 2 under El Centro earthquake ground motion

Fig. 5 shows the time histories of the structural responses of the bridge (segment 2) under scaled El Centro earthquake ground motion when pounding has not been considered in the analysis. It can be seen that the maximum displacement and acceleration response of the segment are 0.143 m and 9.60 m/s^2. The relative displacement between adjacent segments is well above the spacing between the adjacent segments.

The dynamic responses of the uncontrolled bridge model with pounding effects by applying the contact point under El Centro earthquake are also shown in Fig. 5. It can be observed that several sharp peaks appear in the time history responses due to pounding with the application of contact point. The segment has been subjected to several collisions on the left- and right side of the segment, as evident in Fig. 5. The peak displacement of the response has been reduced from 0.143 m to 0.126 m. However, maximum acceleration of the segment has been increased nearly four times from 8.56 m/s^2 to 33.87 m/s^2. The maximum pounding forces on the left and right side of the segment have been observed to be 68.29 and 65.59 MN. Such pounding forces are capable of causing significant damage to the bridge model considered herein.

4.4 Response of the bridge with control by MR damper

The advantages of the application of MR damper in reducing pounding effect have been investigated. The bridge has been analysed for three control strategies- passive off, passive on, and bang-bang control. As mentioned in Section 3.2, the current is held at the constant values of 0 and 2 V for passive off and passive on MR dampers, respectively.

Figs. 6-8 represent the time histories of the structural responses of the bridge under scaled El Centro earthquake ground motion for the three control strategies adopted herein. The dynamic responses of the bridge in the form of peak values of have been reported in Table 2.

It can be observed from Fig. 6 that peak displacement of the bride segment has been reduced from 0.126 m to 0.101 m, providing a 20% reduction with the installation of passive off MR damper when compared with uncontrolled response of the bridge segment. Similarly peak acceleration of the bridge segment has been reduced from 33.87 m/s^2 to 27.87 m/s^2. The reduction is about 18% (Table 2). Left side pounding and right side pounding of the segment have been reduced from 68.29 MN to 53.01 MN and 65.59 MN to 50.22 MN. The achieved reductions are well above 20%.

Fig. 7 reveals that structural response of the bridge segment can be significantly suppressed by the installation of passive on MR damper. The peak displacement and acceleration of the bridge segment have been reduced from 0.126 m to 0.077 m and 33.87 m/s^2 to 18.25 m/s^2, providing reductions of 39% and 46% respectively (Table 2). Also, left side and right side pounding force have been reduced from 68.29 MN to 42.66 MN and 65.59 MN to 52.23 MN. The reductions are 38% and 20%, respectively.

Fig. 8 represents the structural response of the bridge with the installation of MR damper acting on simple control strategy termed as bang-bang control. It is important to note that the maximum input current has been considered as 2 V, similar to passive on MR damper. Slightly improved performance in the reduction of pounding force has been observed with the adopted simple control strategy. The peak displacement and acceleration of the bridge segment have been reduced from 0.126 m to 0.077 m and 33.87 m/s^2 to 20.25 m/s^2, providing reductions of 39% and 40% respectively (Table 2). Left side and right side pounding force have been reduced from 68.29 MN to 37.01 MN and 65.59 MN to 44.05 MN. The reductions are 46% and 33%, respectively.

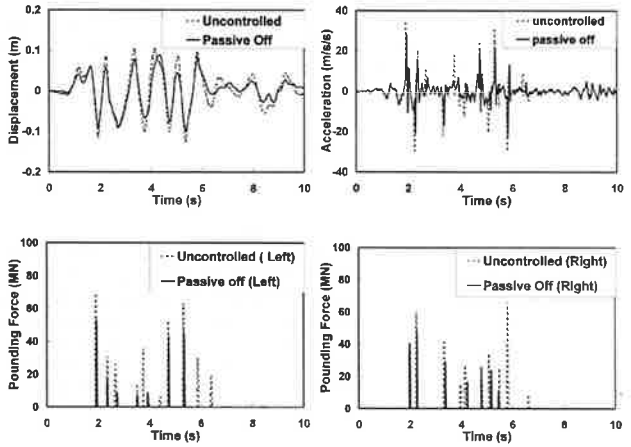

Fig. 6 Structural response of bridge (segment 2) with MR damper (passive off) under El Centro earthquake ground motion

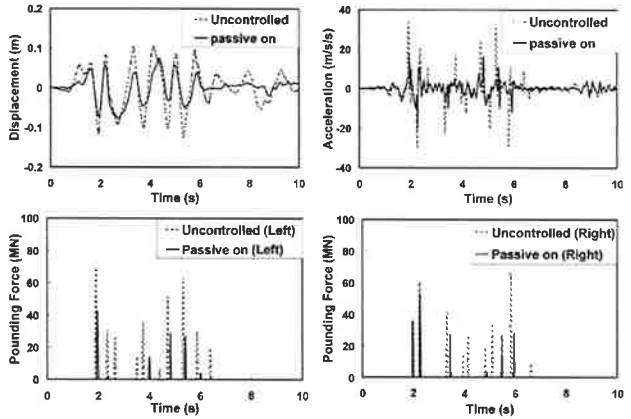

Fig. 7 Structural response of bridge (segment 2) with MR damper (passive on) under El Centro earthquake ground motion

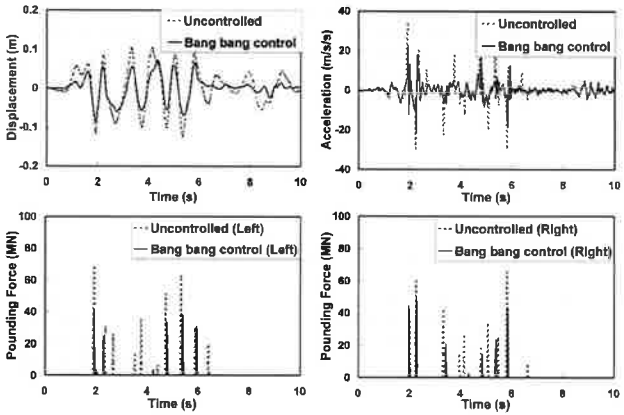

Fig. 8 Structural response of bridge (segment 2) with MR damper (bang bang control) under El Centro earthquake ground motion

Table 2 Response of the bridge (segment 2) with MR damper under El Centro earthquake ground motion

Earthquake Record	Response Quantity	Control of MR damper			
		Without control	Passive off	Passive on	Bang-bang control
The El Centro Earthquake	Displacement (m)	0.105	0.088 (17%)	0.075 (29%)	0.064 (39%)
		-0.126	**-0.101**(20%)	**-0.077** (39%)	**-0.077** (39%)
	Acceleration (N/m^2)	**33.87**	**27.87** (18%)	**18.25** (46%)	**20.25** (40%)
		-29.78	-22.37 (25%)	-21.76 (27%)	-18.83 (37%)
	Left side of pounding force (MN)	**68.29**	**53.01** (22%)	**42.66** (38%)	**37.01** (46%)
		-14.9	-10.85 (27%)	-5.57 (63%)	-6.28 (58%)
	Right side of pounding force (MN)	**65.59**	**50.22** (23%)	**52.32** (20%)	**44.05** (33%)
		-14.03	-10.6 (24%)	-10.74 (23%)	-8.79 (37%)

N.B. Bold fonts represent absolute maximum response quantities. Values with bracket represent percentage of reductions. Positive values indicate response in the direction of ground motion and negative values represent response opposite to the direction of ground motion.

It can be observed from the analysis (Figs. 6-8 and Table 2) that peak displacement, acceleration, and pounding forces can be significantly reduced by the installation of MR damper, although pounding forces have not been mitigated fully. It is important to note that the scaled El Centro ground motion is representative of very strong earthquake ground motion. The pounding effect

could be completely mitigated if the analysis were conducted for moderate earthquake ground shaking levels. All three control strategies have been found to be effective in reducing pounding force generated due to collision between adjacent segments as a result of velocity exchange. Pounding of bridge model has been observed to be reduced to some extent with the installation of passive off MR damper, which mainly provides additional damping to the model. However, due to low energy dissipation ability, considerable pounding force has been observed for the analysed bridge. Passive on MR damper has been observed to be effective in reducing peak displacement and acceleration response of the bridge. Also, significant reduction of pounding force has been achieved with the installation of passive on MR damper. Improved performance has been observed with the installation of MR damper adopting the bang-bang control strategy. It is recommended that the study be extended to investigate other control strategies which might be able to reduce or mitigate the pounding force more effectively.

5. Conclusions

Bridges are considered critical components of highway transportation system; however, recent earthquakes have demonstrated their vulnerability even in the event of a moderate level of earthquake ground motion. Pounding between superstructure segments is considered one of the main reasons for damage and collapse of base-isolated multi-span RC highway bridges.

A simplified analytical model in conjunction with MR damper for pounding between adjacent superstructure segments has been developed. Linear visco-elastic contact element approach has been chosen to model seismic pounding effect, as the parameter selection and numerical solution is easier and transparent in such approach.

Analysis of a three-segment bridge shows that seismic pounding can generate significant force which may cause damage at the point of collision. Acceleration of superstructure segment due to pounding has been observed to be amplified by several times.

It has been observed that seismic pounding effect can be effectively reduced by MR damper. Three control strategies namely, passive off, passive on, and bang-bang control have been investigated. The pounding of the superstructure segment can be reduced by passive-off control strategy to some extent due to their low energy dissipation ability. In the case of passive on control strategy, the pounding between adjacent superstructure segments has been reduced effectively. However, with a simple control algorithm, bang bang control has been found to be the most effective.

References

Anagnostopoulos, S.A. (1988), Pounding of building in series during earthquake", *Earthq. Eng. Struct. D.*, **16**(3), 443-456.

Jung, H.J., Jang, D.D., Choi, K.M. and Cho, S.W. (2009), "Vibration mitigation of highway isolated bridge using MR damper-based smart passive control system employing an electromagnetic induction part", *Struct. Contol Hlth. Monit.*, **16**(6), 613-625.

Guo, A.X. and Li, H. (2008), "Pounding reduction of highway bridges with pounding effect by using Magnetorheological dampers under earthquake excitation", *Adv. Struct. Eng.*, **11**(3), 317-334.

Guo, A.X., Li, Z., Li, H. and Ou, J. (2009), "Experimental and analytical study on pounding reduction of base-

isolated highway bridges using MR dampers", *Earthq. Eng. Struct. D.*, **38**(11), 1307-1333.
Jankowski, R., Wilde, K. and Fujino, Y. (1998), "Pounding of superstructure segments in isolated elevated bridge during earthquakes", *Earthq. En. Struct. D.*, **27**, 487-502.
Jankowski, R., Wilde, K. and Fujino, Y. (2000), "Reduction of pounding effects in elevated bridges during earthquake", *Earthq. Eng. Struct. D.*, **29**(2), 195-212.
Li, W.H., Du, H., Chen, G., Yeo, S.H. and Guo, N.Q. (2002), "Nonlinear rheological behavior of magnetorheological fluids: step-strain experiments", *Smart Mater. Struct.*, **11**(2), 209-217.
Li, W.H., Yao, G.Z., Chen, G., Yeo, S.H. and Yap, F.F. (2000), "Testing and steady state modeling of a linear MR damper under sinusoidal loading", *Smart Mater. Struct.*, **9**(1), 95-102.
Maison B.F. and Kasai, K. (1990), "Analysis for type of structural pounding", *J. Struct. Eng.*, **116**, 957-977.
Sireteanu, T. and Stammers, C.W. (2000), "Control of building seismic response by means of three semi-active friction dampers", *J. Sound Vib.*, **237**(5), 745-759.
Spencer B.F., Dyke, S.J., Sain, M.K. and Carlson, J.D. (1997), "Phenomenological model of a magnetorheological damper", *J. Eng. Mech.*, **123**(3), 230-238.
Vega, J., Rey, I.D. and Alarcon, E. (2009), "Pounding force assessment in performance-based design of bridges", *Earthq. Eng. Struct. D.*, **38**, 1525-1544.
Wang, X. and Gordaninejad, F. (2007), *Magnetorheological Materials and Their Applications, Intelligent Materials*, Eds. Shahinpoor, M. and Schneider, H.J., 339-385.
Yang, M.G., Chen, Z.Q. and Hua, X.G. (2011), "An experimental study on using MR damper to mitigate longitudinal seismic response of a suspension bridge", *Soil Dyn. Earthq. Eng.*, **31**, 1171-1181.
Yao, G.Z., Yap, F.F., Chen, G., Li, W.H. and Yeo, S.H. (2002), "MR damper and its application for semi-active control of vehicle suspension system", *Mechatronics*, **12**(7), 963-973.
Zhu, P., Abe, M. and Fujino, Y. (2004), "Evaluation of pounding countermeasures and serviceability of elevated bridges during seismic excitation using 3D modeling", *Earthq. Eng. Struct. D.*, **33**(5), 591-609.